JSC-08682

**NASA TECHNICAL MEMORANDUM**

NASA TM X-58129
February 1974
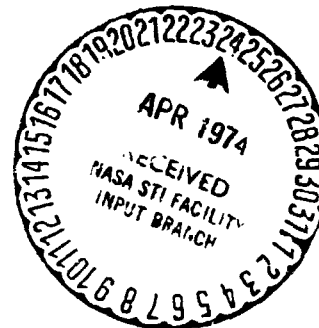
**MEASUREMENT OF ATMOSPHERIC PRECIPITABLE WATER**

**USING A SOLAR RADIOMETER**

**NATIONAL AERONAUTICS AND SPACE ADMINISTRATION**

**LYNDON B. JOHNSON SPACE CENTER**

**HOUSTON, TEXAS 77058**

# MEASUREMENT OF ATMOSPHERIC PRECIPITABLE WATER

# USING A SOLAR RADIOMETER

David E. Pitts and William McAllum
Lyndon B. Johnson Space Center
Houston, Texas 77058

Alyce E. Dillinger
Lockheed Electronics Co.
Houston, Texas 77058

# CONTENTS

## TABLE

## FIGURES

# MEASUREMENT OF ATMOSPHERIC PRECIPITABLE WATER

## USING A SOLAR RADIOMETER

By David E. Pitts, William McAllum, and Alyce E. Dillinger[*]
Lyndon B. Johnson Space Center

## SUMMARY

Measurements of total atmospheric water vapor are accomplished by ratioing a water-vapor absorbing region (0.9435 micrometer) to a clear channel (0.8730 micrometer). Aerosol extinction is usually a slowly varying function of wavelength in the visible and near infrared. This ratioing effectively eliminates the aerosol and Rayleigh scattering leaving only the water-vapor absorption effects. Because a small amount of water vapor may saturate the strong water bands and a large amount of water vapor may not saturate the weak bands, this ratio is neither a linear nor an exponential function of precipitable water.

## INTRODUCTION

The purpose of this paper is to describe a method of using a solar radiometer to deduce precipitable water in the atmosphere. The technique uses two channels. One channel covers a water-vapor absorption region, and the other, a nearby region in which water-vapor absorption is absent. The method operates on the assumption that the aerosol and Rayleigh scattering optical depths are approximately the same in the two channels. This assumption allows the ratio of the two channels to be used to eliminate the aerosol and Rayleigh scattering and thus gives the precipitable water in the slant path. By dividing the water amount by the air mass,[1] the precipitable water[2] in the vertical path may be obtained. Such an instrument was reportedly constructed and calibrated against radiosonde data during the early 1960's, but the details of the instrument and its success have not been verified.[3]

---

[*]Lockheed Electronics Co., Houston, Texas 77058.

[1]The air mass is defined as the secant of the angle from the zenith.

[2]Precipitable water (centimeters) is defined as the total amount of water vapor (grams) in a column above a surface area of 1 square centimeter, divided by the density of liquid water (ref. 1).

[3]Murcray and Barker (ref. 2) accredited Foster, Volz, and Foskett with the successful construction and calibration of this instrument.

$A = 0.416$

$B = -1.01 \times 10^{-3} \; (\mu m)^{-2}$

$C_1, C_2$      constants

$$C_3 = \frac{I_{o,\nu_{1,2}} C_1 \int_3^4 F_2(\nu) d\nu}{I_{o,\nu_{3,4}} C_2}$$

$F_1$      $\phi(\lambda)$ of channel 1

$F_2$      $\phi(\lambda)$ of channel 2

$$F_2(\nu) = A \; \exp\left[B\left(\lambda - \lambda_o\right)^2\right]$$

$I$      intensity $(W/cm^2 \; \mu m \; sr)$

$\bar{I}$      average intensity

$I_o$      downwelling known intensity

$J$      meter reading of solar radiometer for air mass $m$

$J_o$      meter reading of solar radiometer for air mass $m = 0$

$K$      experimentally determined constant $= 0.422$

$K_\nu$      absorption coefficient of the gas at frequency $\nu$

$m$      air mass $= \sec \theta$ (an approximation valid 3 percent for $0^o \le \theta \le 80^o$) $= 1/\mu$

$P_o$      precipitable water (cm) in the vertical path

$T$      atmospheric transmission

$\bar{T}$      average atmospheric transmission

2

| | |
|---|---|
| $T(\lambda)$ | atmospheric transmission as a function of wavelength |
| $T_4$ | atmospheric transmission for radiometer unit 4 |
| $\bar{T}_u$ | atmospheric transmission for uncalibrated radiometer |
| $z$ | altitude in the atmosphere |
| $\theta$ | zenith angle |
| $\lambda$ or $\nu$ | wavelength or frequency, respectively |
| $\lambda_o$ or $\nu_o$ | center wavelength (0.9435 μm) or frequency (10 598.83 $cm^{-1}$), respectively |
| $\mu$ | cos $\theta$ |
| $\rho$ | atmospheric density |
| $\rho_{H_2O}$ | density of water at standard temperature and pressure |
| $\tau$ | optical depth |
| $\tau_o$ | optical depth of entire atmosphere |
| $\phi(\lambda)$ | least-squares fit of the transmission of the solar radiometer filter |

Superscripts:

| | |
|---|---|
| $-$ | downwelling quantity |
| $x$ | experimentally determined constant = 0.574 |

Subscripts:

| | |
|---|---|
| 1,2 | quantity over limits 1 to 2 |
| 3,4 | quantity over limits 3 to 4 |
| 0.9420 | quantity at 0.9420 μm |
| 0.8730 | quantity at 0.8730 μm |
| a | atmospheric gaseous absorption processes |
| b | black-body radiator at a specified temperature |

s           atmospheric Rayleigh and aerosol extinction

t           dummy variable

## RADIOMETER MEASUREMENTS AND ACCURACY

Atmospheric aerosol and molecular scattering and absorption by atmospheric gases are deleterious conditions that distort the upwelling terrestrial radiation and cause problems in the automatic classification of multispectral imagery by automatic pattern recognition techniques (refs. 3 and 4). Moreover, these atmospheric conditions have large temporal and spatial variations that may require atmospheric corrections to be made over a grid covering the field of view of the remote sensor. For example, large gradients of precipitable water exist across dry fronts in the Midwest. These gradients may cause variations in precipitable water of from 1.9 to 3.0 centimeters over a distance of 40 kilometers (ref. 1). To allow for such atmospheric variations, a seven-channel Sun radiometer for measuring the optical depth of the atmosphere was designed, constructed, and tested in the field for more than a year (fig. 1). This unit is similar to the Volz Sun photometer used by Flowers et al. (ref. 5) and Volz (ref. 6) in 43 cities in the United States to determine atmospheric turbidity for air quality monitoring and is also similar to the multiple wavelength radiometer described by Shaw et al. (ref. 7). To distinguish between different types of aerosols (e.g., continental and maritime), Reeser (refs. 8 and 9), and Kleen (ref. 10) determined that it was necessary to measure atmospheric extinction at multiple wavelengths.

A device was needed to adequately measure such atmospheric extinction and to cover the principal visible and near infrared bands of the Earth Resources Technology Satellite (ERTS) multispectral scanner (MSS) (ref. 11) and the Earth Resources Experiment Package (EREP) multispectral scanner (ref. 12). An analysis (ref. 13) was made that indicated an optimum set of wavelengths (0.38, 0.50, 0.61, 0.7487, 0.8730, and 1.04 micrometers) that could be used to meet this need. A study of the accuracy of the operator-radiometer-atmosphere system revealed a ±10-percent error in measurements of the aerosol optical depth. An additional band at 0.9435 micrometer was chosen to measure absorption caused by atmospheric water vapor.

Kleen (ref. 10) showed that by ratioing the meter reading in the 0.9435-micrometer band to the meter reading in the 0.8730-micrometer band, the water-vapor absorption could be measured. The band at 0.8730 micrometer was chosen over that at 1.04 micrometers because the former is closer to the peak response of the silicon detector used in the radiometer. A network of these radiometers in the field of view of the ERTS or EREP multispectral scanners will give a small-scale picture of both aerosol and water-vapor effects on traversing signals. However, a more practical operational scheme that uses spacecraft data for this purpose will have to be developed to facilitate pattern recognition of large or remote areas of the world.

4

Cousin et al. (ref. 14) have described the method (the Prediction of Response of Earth Pointed Sensors-Reconstruction of Target Reflectance (PREPS-ROTAR)) for using these data to correct multispectral scanner data from ERTS at bands of 0.5 to 0.6, 0.6 to 0.7, 0.7 to 0.8, and 0.8 to 1.1 micrometers for aerosol effects using a table look-up scheme based on a solution to the radiative transfer equation known as the doubling method (refs. 15 and 16). With the calibration of the water channel of one solar radiometer represented by this paper, the other 16 radiometers may be cross-calibrated. The precipitable water obtained may then be used as an input, and water-vapor absorption effects may be removed from bands at other wavelengths for ERTS, EREP, or aircraft data with a similar look-up table. This look-up table was generated by modifying a compressed line-by-line atmospheric transmission model by Deutschman and Calfee (ref. 17) by using a set of atmospheric soundings to represent an extreme range of atmospheric precipitable water over extremes in temperature and moisture distributions (ref. 1). These results will then be included in the PREPS-ROTAR correction program. (A paper describing this look-up table for the ERTS MSS7 (0.8 to 1.1 micrometers) and the effect of water vapor on signature extension for corn and soybeans is being prepared by the authors as a companion paper.)

## CALIBRATION OF THE SOLAR RADIOMETER

Atmospheric transmission $T(\lambda)$ for the 0.9435-micrometer water band was calculated by using a least-squares fit of the transmission of the filter for solar radiometer unit 4, as determined from a spectrophotometer (fig. 2). The Gaussian function $\phi(\lambda)$ used for the fit was of the form

$$\phi(\lambda) = A \exp\left[B\left(\lambda - \lambda_o\right)^2\right] \tag{1}$$

Because the spectral response of the silicon detector changes by less than 0.5 percent and the solar irradiance changes by less than 2 percent over the width of the filter function, it was not necessary to include these terms in calculating the average transmission $\bar{T}$ for the band from the atmospheric transmission $T(\lambda)$.

$$\bar{T} = \frac{\displaystyle\int_{0.935}^{0.950\mu m} T(\lambda)\phi(\lambda)d\lambda}{\displaystyle\int_{0.935}^{0.950\mu m} \phi(\lambda)d\lambda} \tag{2}$$

5

The integrals in equation (2) were evaluated using the Simpson rule, incorporating atmospheric transmissions obtained for a 10-layer atmospheric model, and calculating water-vapor absorption with about 1 centimeter$^{-1}$ accuracy (fig. 3) smoothed by a triangular filter function 20 centimeters$^{-1}$ wide at the base (fig. 4). Values were calculated for 10 radiosonde data sets (ref. 1) representing a range of 0.166 to 5.851 centimeters precipitable water (fig. 5). This information includes the extreme range of precipitable water observed in the United States over a 9-month period in 1972 and 1973.

The solution for a downwelling known intensity $I_o$, such as the Sun passing through an absorbing atmosphere where no scattering occurs, is

$$\bar{I}_{va}\left(\tau_{va},\mu\right) = I_{ov}e^{\frac{\tau_{va}-\tau_{o,va}}{\mu}} + \frac{1}{\mu}\int_{\tau_{va}}^{\tau_{o,va}} e^{\frac{\tau-t}{\mu}} I_{bv(t)}\, dt \qquad (3)$$

However, if the atmosphere does not radiate strongly at the wavelengths considered and measurements are made at the Earth surface $\tau_{va} = 0$, equation (3) simplifies to

$$\bar{I}_{va}(0,\mu) = I_{ov}e^{-\tau_{o,va}/\mu} \qquad (4)$$

Now, if single scattering without an absorptive process is considered, a similar expression can be derived as a solution to the radiative transfer equations (ref. 18)

$$\bar{I}_{vs}(0,\mu) = I_{ov}e^{-\tau_{o,vs}/\mu} \qquad (5)$$

If these two processes are visualized as distinct phenomena with each occurring in a separate mathematical layer representative of the real atmosphere where both phenomena occur, then the total intensity transversing the layers is

$$\bar{I}_{v}(0,\mu) = \bar{I}_{vs}(0,\mu)\bar{I}_{va}(0,\mu) \qquad (6)$$

6

or

$$\bar{I}_{\nu sa}(0,\mu) = I_{o\nu}e^{\left(-\tau_{o,\nu s}/\mu\right)-\left(\tau_{o,\nu a}/\mu\right)} \tag{7}$$

Now, if the solar intensity is measured in two bands, one with aerosol and water-vapor absorption and one with only aerosol absorption, if finite filter functions $F_1$ and $F_2$ are used for each, and if $I_{o\nu}$ is a slowly varying function between $\nu_1$ to $\nu_2$ and $\nu_3$ to $\nu_4$, then equation (5) becomes

$$\bar{I}_{\nu s}(0,\mu) = \frac{I_{o,\nu}}{1,2}\frac{\displaystyle\int_{\nu_1}^{\nu_2} F_1(\nu)e^{-\frac{\tau_{o,\nu,s}}{\mu}}d\nu}{\displaystyle\int_{\nu_1}^{\nu_2} F_1(\nu)d\nu} \tag{8}$$

and equation (7) becomes

$$\bar{I}_{\nu sa}(0,\mu) = \frac{I_{o,\nu}}{3,4}\frac{\displaystyle\int_{\nu_3}^{\nu_4} F_2(\nu)e^{-\frac{\tau_{o,\nu,s}}{\mu}}e^{-\frac{\tau_{o,\nu,a}}{\mu}}d}{\displaystyle\int_{\nu_3}^{\nu_4} F_2(\nu)d\nu} \tag{9}$$

where $\nu_1$ to $\nu_2$ covers the 0.8730-micrometer band and $\nu_3$ to $\nu_4$ covers the 0.9420-micrometer water band. Now, if aerosol optical depth $\tau_{o,\nu,s}$ is a slowly varying function of frequency over the range of frequencies $\nu_1$ to $\nu_4$,

then $e^{-\tau_{o,\nu,s}}$ can be removed from the integrals in equations (8) and (9) so that the ratio of equations (8) and (9) gives

$$\frac{\bar{I}_{\nu sa}(0,\mu)}{\bar{I}_{\nu s}(0,\mu)} = \frac{I_{o,\nu_{3,4}} \displaystyle\int_{\nu_3}^{\nu_4} F_2(\nu)e^{-\frac{\tau_{o,\nu,a}}{\mu}}\,d\nu}{I_{o,\nu_{1,2}} \displaystyle\int_{\nu_3}^{\nu_4} F_2(\nu)\,d\nu} \tag{10}$$

where $F_2$ is the filter function over the water band $\nu_3$ to $\nu_4$. Now, since $\bar{I}_{\nu sa}(0,\mu) = C_1 J_{(0.9420)}$ and $\bar{I}_{\nu s}(0,\mu) = C_2 J_{(0.8730)}$, then equation (10) becomes

$$C_3 \frac{J_{(0.9420)}}{J_{(0.8730)}} = \int_{\nu_3}^{\nu_4} F_2(\nu)e^{-\left(\tau_{o,\nu,a}\right)^m}\,d\nu \tag{11}$$

where $F_2(\nu) = A \exp[B(\lambda - \lambda_o)^2]$. Furthermore

$$\tau_{o,\nu,a} = \int_0^z K_\nu \rho \, dz \tag{12}$$

For wavelengths near 1.0 micrometer, $K$ is approximately independent of $z$ (i.e., not dependent on temperature) so

$$\tau_{o,\nu,a} = K_\nu P_o \rho_{H_2 O} \tag{13}$$

8

so

$$C \frac{J_{(0.9420)}}{J_{(0.8730)}} = \int_{\lambda_3}^{\lambda_4} \exp\left[+B\left(\lambda - \lambda_o\right)^2 - K_\nu P_o m\right] d\lambda \qquad (14)$$

where $C = \dfrac{C_3}{A} = \dfrac{J_{o(0.8730)}}{J_{o(0.9420)}}$. Numerical evaluations of the preceding integral show that it is of the form $\exp(-KP_o^x m^x)$ so that

$$\frac{J_{o(0.8730)}}{J_{o(0.9420)}} \frac{J_{(0.9420)}}{J_{(0.8730)}} = \exp\left(-KP_o^x m^x\right) \qquad (15)$$

if the ratio $J_{c(0.8730)}/J_{o(0.9420)}$ now includes the terms $C_3/A$.

The water-vapor transmission is not an exponential function of precipitable water (fig. 5). This fact indicates that the transmission does not obey Beer's law. This is because the centers of strong bands saturate at low water amounts, leaving the weak absorbing lines to contribute to additional absorption. The ad hoc function

$$\bar{T} = \exp\left(-KP_o^{\hat\kappa} m^x\right) \qquad (16)$$

was determined to represent a good fit to the curve in figure 5 for solar radiometer unit 4.

Equations (14) and (15) assume the optical depth for aerosol and Rayleigh scattering is approximately the same in these adjacent channels. The Rayleigh optical depth changes by about a factor of 2 for these wavelengths, but it is a very small value of approximately $0.01 \pm 10$ percent, whereas the aerosol optical depth is about 0.5 (ref. 18).

Radiosonde data from downtown Houston, Texas, and solar radiometer data from the NASA Lyndon B. Johnson Space Center (JSC) at Clear Lake City, Texas, were collected for the same days. The ratio of $J_{(0.9435)}/J_{(0.8730)}$ was compared to the precipitable water amounts from the radiosonde data in figure 5 and gave a subjective best fit of 0.44 for the value of $[J_{o(0.8730)}/J_{o(0.9435)}]_4$ that represented the curve adequately except at higher water

amounts. These anomalous values are very likely attributable to the higher
moisture amounts present at JSC, which is 40 kilometers southeast of the
downtown Houston area where the 0600 l.s.t. radiosonde is launched. Most solar
radiometer measurements are made at 0900 to 1100 l.s.t. when the sea breeze is
starting to penetrate the coastal areas.

Once the calibration value $[J_{o(0.8730)}/J_{o(0.9435)}]_4$ is known for radiom-
eter unit 4, the meter readings $J_{(0.9435)}$ and $J_{(0.8730)}$ from radiometer
unit 4 can be used to obtain the transmission in the water band $\bar{T}$, which allows
the precipitable water in the slant path to be calculated using the curve in
figure 5. Dividing the precipitable water in the slant path by the air mass
(sec $\theta$) will give the precipitable water in the vertical path.

Precipitable water measurements using other radiometers may be obtained by
taking the ratio of the measurements $J_{(0.9435)}/J_{(0.8730)}$ and multiplying by
the calibration value $J_{o(0.8730)}/J_{o(0.9435)}$ for the appropriate radiometer
from table I.

Figure 6 will then relate this calculated value to precipitable water in
the slant path. The precipitable water in the vertical path may be obtained by
dividing the slant path amount by the air mass m.

Because each filter has a slightly different transmission function, the
response of transmission as compared to precipitable water is different for the
0.9435-micrometer band of each radiometer. Figure 6 shows the calibration
curves for all 17 radiometers. The curves were obtained by integrating the
measured filter response functions over the absorption caused by water atmos-
pheric vapor; five different atmospheric profiles were used in the same manner
as just described for radiometer unit 4. Many of the curves are, for practical
purposes, identical.

Once the calibration values $[J_{o(0.8730)}/J_{o(0.9435)}]_4$ are known for the
radiometer unit 4, calibration of the other units that were available were un-
dertaken by making simultaneous measurements with radiometer unit 4 and the un-
known radiometer. The technique used for finding the calibration values
$[J_{o(0.8730)}/J_{o(0.9435)}]$ for the uncalibrated radiometers is as follows:

1. Obtain two sets of simultaneous readings with radiometer unit 4 and
the unknown instrument for the 0.8730- and 0.9435-micrometer channels. The two
sets should be compared to eliminate reading or writing errors.

2. Use $[J_{o(0.8730)}/J_{o(0.9435)}]_4$ for the calibrated photometer and the
measured values $[J_{(0.9435)}/J_{(0.8730)}]_4$ for the calibrated photometer to cal-
culate $\bar{T}_4$, where $\bar{T}_4 = 0.44[J_{(0.9435)}/J_{(0.8730)}]_4$.

3. Use figure 6 to calculate precipitable water in the slant path based on measurements from radiometer unit 4.

4. Use the precipitable water from step 3 to find the transmission for the uncalibrated radiometer $\bar{T}_u$ using figure 6.

5. Use measured values $J_{(0.9435)}$ and $J_{(0.8730)}$ from the uncalibrated radiometer and the $\bar{T}_u$ from step 4 to calculate the calibration constants $J_{o(0.8730)}/J_{o(0.9435)}$.

$$\frac{J_{o(0.8730)}}{J_{o(0.9435)}} = \frac{J_{(0.8730)}}{J_{(0.9435)}} \bar{T}_u \tag{17}$$

Table I gives calibration values obtained in this manner for all radiometers that were available in the summer of 1973.

6. Obtain a second set of simultaneous measurements on a different day, perform steps 1 through 5, and cross correlate the values of water obtained with radiometer unit 4 and the instrument being calibrated. Figure 7 is an example of such a calibration verification.

If radiometer unit 4 becomes uncalibrated, units 1, 2, or 3 should be used as the standard.

In several studies, Morrissey and Brousaides (ref. 19), Barnes et al. (ref. 20), and others discuss temperature-induced errors in humidity, problems in repetition, and problems with response of radiosondes that served as the standard for measurement of water vapor for this technique. Brousaides and Morrissey (refs. 21 and 22) discuss an improvement in the radiosonde that eliminates the systematic trend to measure drier daytime profiles than infrared and other water-vapor measurements in the Barbados Oceanographic and Meteorological Experiment project. Their redesign of the radiosonde that was implemented by the National Oceanic and Atmospheric Administration in 1972 shows an increase of 30 percent relative humidity (e.g., from 50 to 80 percent relative humidity) for some cases above $500 \times 10^2$ $\Gamma/m^2$ (500 millibars). All the data used in this report were from the improved radiosonde system.

According to Brousaides (ref. 23), most radiosondes have laboratory accuracies of ±3 percent or less for relative humidity at temperatures above 298 K; however, at temperatures below 253 K, the error increases to ±6 percent with a mean bias of as much as 7 percent. However, at present, no assessment of the absolute accuracies for temperature and relative humidity is available to calculate the accuracy of determining total water from radiosonde data.

Water vapor is one of the most highly variable of all atmospheric constituents; thus, the accuracy of calibrating a solar radiometer by a balloon-launched

sensor requiring tens of minutes to measure . rofile will always be limited. It is the authors' opinion that the relative midity measurement from the radiosonde is accurate to about ±10 percent for values of relative humidity greater than 20 percent. If absolute radiance could be derived for the two channels of the radiometer, the accuracy of the radiosonde would no longer be the limiting factor in determining precipitable water in the atmosphere.

## CONCLUDING REMARKS

The technique of using the solar radiometer allows a self-consistent measurement of precipitable water to be made that can be used as an input to a transmission look-up table for other spectral bands of water-vapor absorption. As such, precipitable water serves as a convenient, physically meaningful, intermediary quantity.

Lyndon B. Johnson Space Center
   National Aeronautics and Space Administration
      Houston, Texas, February 26, 1974
         951-16-00-00-72

# REFERENCES

1. Jeske, K. W.: Extreme Atmosphere Models, 1973. NASA TM X-58112, 1974.

2. Murcray, D. G.; and Barker, D. B.: Balloon Borne Humidity and Aerosol Sensors. NASA CR-61?39, Feb. 1971.

3. Anon.: Remote Multispectral Sensing in Agriculture. Res. Bull. No. 844, Laboratory for Remote Sensing, Vol. 3, Annual Report, Purdue Univ., Sept. 1968.

4. Bauer, Marvin E.; and Cipra, Jan E.: Identification of Agricultural Crops by Computer Processing of ERTS MSS Data. Symposium on Significant Results Obtained From the Earth Resources Technology Satellite-1, Vol. I: Technical Presentations, Sec. A, Stanley C. Freden, Enrico P. Mercanti, and Margaret A. Becker, compilers and eds., NASA SP-327, 1973, pp. 205-212.

5. Flowers, E. C.; McCormick, R. A.; and Kurfis, K. R.: Atmospheric Turbidity Over the United States, 1961-1966. J. Appl. Meteorol., vol. 8, no. 6, Dec. 1969, pp. 955-962.

6. Volz, F. E.: Some Results of Turbidity Networks. Tellus, vol. ..Ι, Air Force Cambridge Research Laboratories, Nov. 1968, pp. 625-629.

7. Shaw, G. E.; Reagan, J. A.; and Herman, B. M.: Investi ions of Atmospheric Extinction Using Direct Solar Radiation Measurements Made With a Multiple Wavelength Radiometer. J. Appl. Meteorol., vol. 12, no. 2, Mar. 1973, pp. 374-380.

8. Reeser, W. K.: Aerosol Size Distribution Detection for PREPS Using Simple Processing Techniques. LEC/HASD 640-TR-091, Lockheed Electronics Co., Inc. (NASA Contract NAS 9-12200), Mar. 1972.

9. Reeser, W. K.: Aerosol Models Used for PREPS. LEC/HASD 640-TR-109, Lockheed Electronics Co., Inc. (NASA Contract NAS 9-12200), May 1972.

10. Kleen, R. H.: Sun Photometer Filter Selection and Gaseous Absorption for PREPS-ERTS-A. LEC/HASD TM 641-471, Lockheed Electronics Co., Inc., Mar. 1972.

11. Anon.: ERTS Data Users Handbook. NASA Technology Satellite, Goddard Space Flight Center, Document 71SD4249, 1972.

12. Anon.: Skylab Experiments. Government Printing Office 3300-0423, Aug. 1972.

13. Reeser, W. K.: A Feasibility Study on the Use of a Sun Photometer in Gathering Aerosol Optical Depth Data for PREPS. LEC/HASD 640-TR-086, Lockheed Electronics Co., Inc. (NASA Contract NAS 9-12200), Mar. 1972.

13

14. Cousin, S. B.; Anderson, A. C.; Paris, J. F.; and Potter, J. F.: Signifi-
    cant Techniques in the Processing and Interpretation of ERTS-1 Data.
    Symposium on Significant Results Obtained From the Earth Resources Tech-
    nology Satellite-1, Vol. I: Technical Presentations, Sec. B, Stanley
    C. Freden, Enrico P. Mercanti, and Margaret A. Becker, compilers and
    eds., NASA SP-327, 1973, pp. 1151-1158.

15. Hansen, James E.: Radiative Transfer by Doubling Very Thin Layers.
    Astrophys. J., vol. 155, no. 2, Feb. 1969, pp. 565-573.

16. Potter, John F.: Scattering and Absorption in the Earth's Atmosphere.
    Proceedings of the Sixth International Symposium on Remote Sensing of
    Environment, Vol. 1, Oct. 13-16, 1969, Willow Run Laboratories, Univ.
    of Michigan, pp. 415-429.

17. Deutschman, Elaine M.; and Calfee, Robert F.: Two Computer Programs to
    Produce Theoretical Absorption Spectra of Water Vapor and Carbon Dioxide.
    Env. Sci. Services Adm. Tech. Rept. IER 31-ITSA 31, Apr. 1967.

18. Elterman, Louis: Vertical-Attenuation Model With Eight Surface Meteoro-
    logical Ranges 2 to 13 Kilometers. Environmental Research Paper 318,
    Air Force Cambridge Research Laboratories, Mar. 1970.

19. Morrissey, James F.; and Brousaides, Frederick J.: Temperature-Induced
    Errors in the ML-476 Humidity Data. J. Appl. Meteorol., vol. 9, no. 5,
    Oct. 1970, pp. 805-808.

20. Barnes, Stanley L.; Henderson, James H.; and Ketchum, Robert J.: Rawi.-
    sonde Observation and Processing Techniques at the National Severe Storm
    Laboratory. NOAA TM ERL NSSL-53, Apr. 1971.

21. Brousaides, F. J.; and Morrissey, J. F.: Improved Humidity Measurements
    With a Redesigned Radiosonde Humidity Duct. Bull. Am. Meteorol. Soc.,
    vol. 9, 1971, pp. 870-875.

22. Brousaides, Frederick J.; and Morrissey, James F.: Residual Temperature-
    Induced Humidity Errors in the National Weather Service Radiosonde,
    Part 1 Instrumentation Paper No. 184, Air Force Cambridge Research
    Laboratories, TR-73-0214, Apr. 1973.

23. Brousaides, Frederick J.: An Assessment of the Carbon Humidity Element
    in Radiosonde Systems. TR-73-0423, Air Force Cambridge Research Lab-
    oratories, 1973

TABLE I.- SOLAR RADIOMETER CALIBRATION VALUES

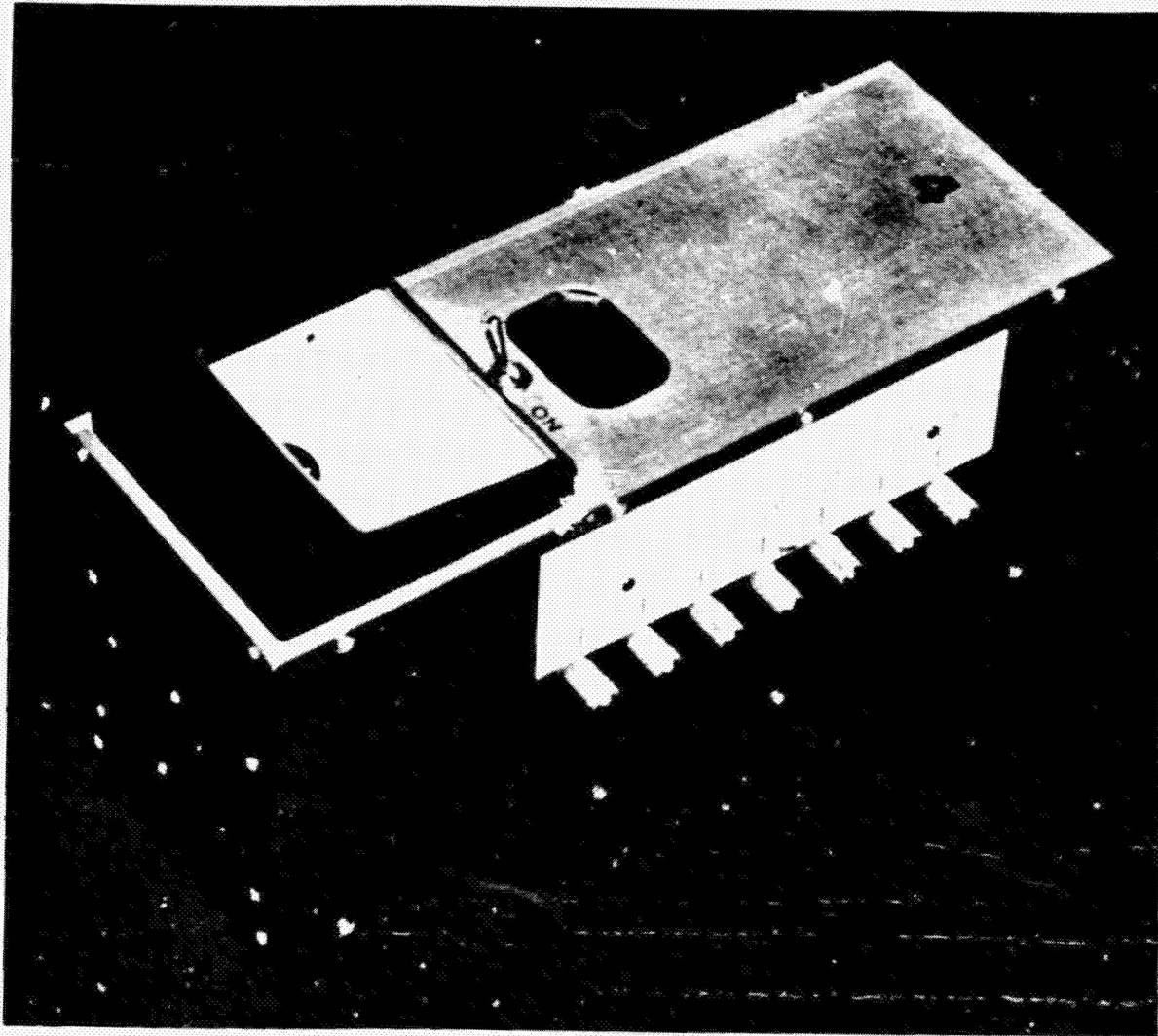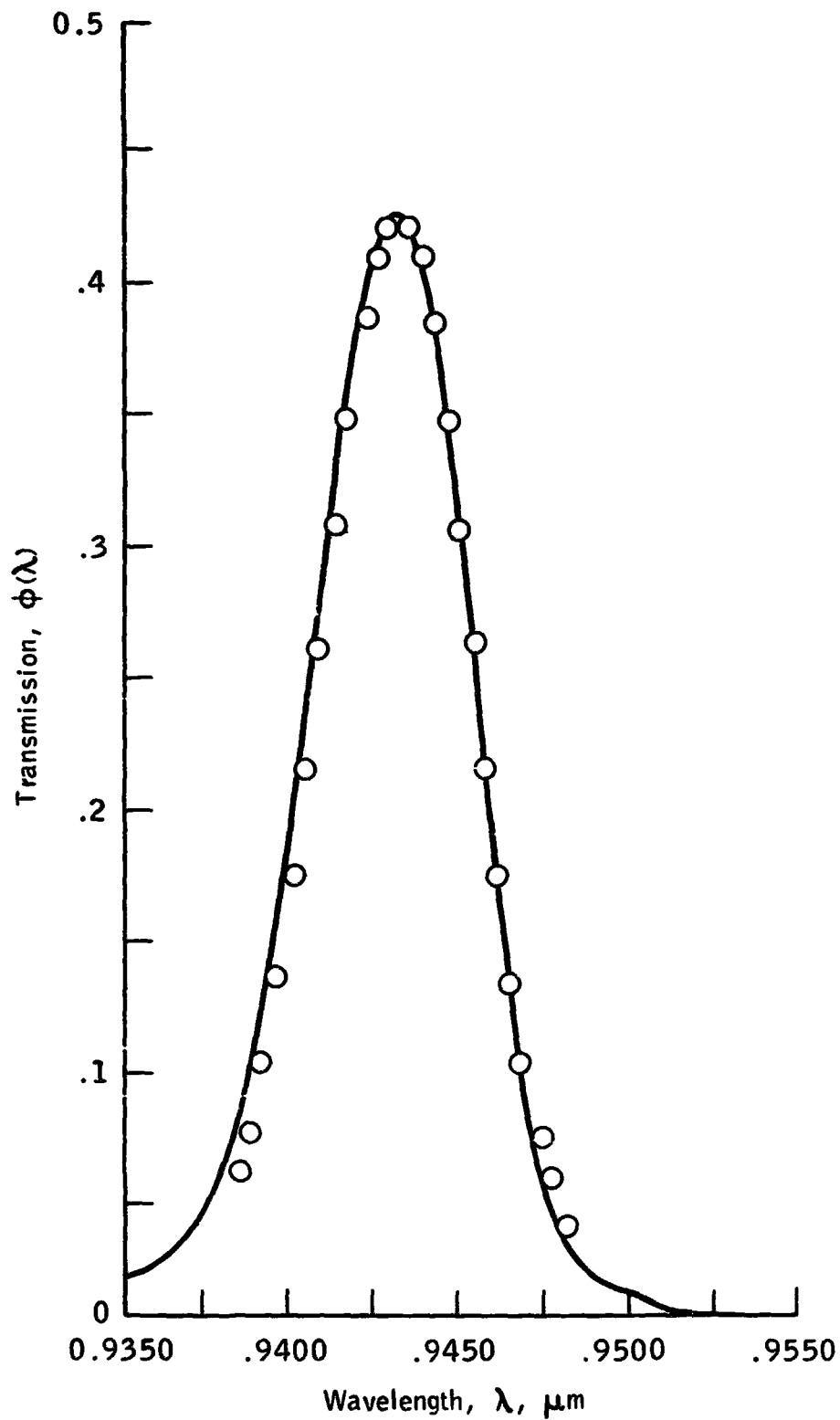| Solar radiometer unit number | Calibration value $\dfrac{J_o(0.8730)}{J_o(0.9435)}$ |
|:---:|:---:|
| 1 | 1.24 |
| 2 | .91 |
| 3 | .67 |
| 4 | .44 |
| 5 | .27 |
| 6 | .381 |
| 7 | .39 |
| 8 | .298 |
| 9 | .30 |
| 10 | .22 |
| 11 | .407 |
| 12 | -- |
| 13 | .284 |
| 14 | .330 |
| 15 | .271 |

Figure 1.- The seven-channel solar radiometer.

Figure 2.- Filter function for the water band for solar radiometer unit 4.
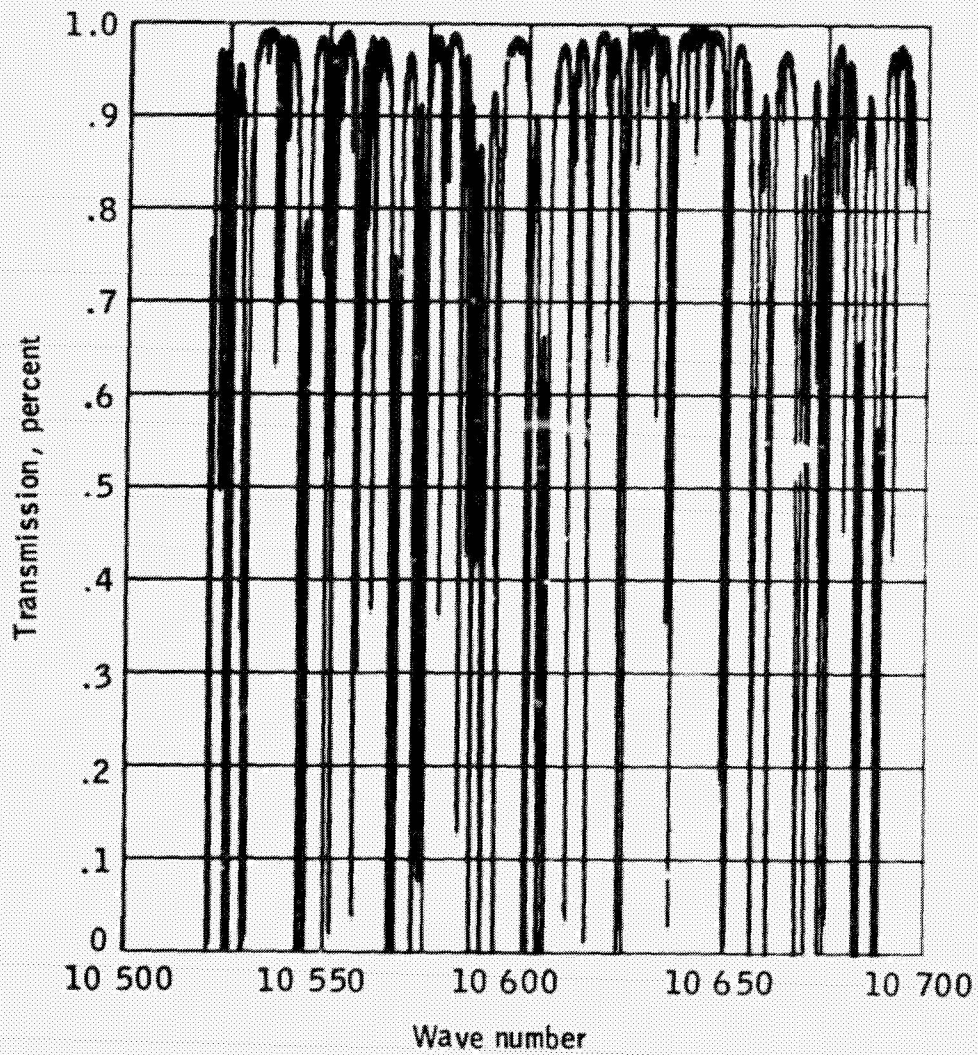
Figure 3.- Calculated transmission through the atmosphere for Albany, N.Y.,
Jan. 10, 1972, radiosonde, 0.202 centimeter precipitable water,
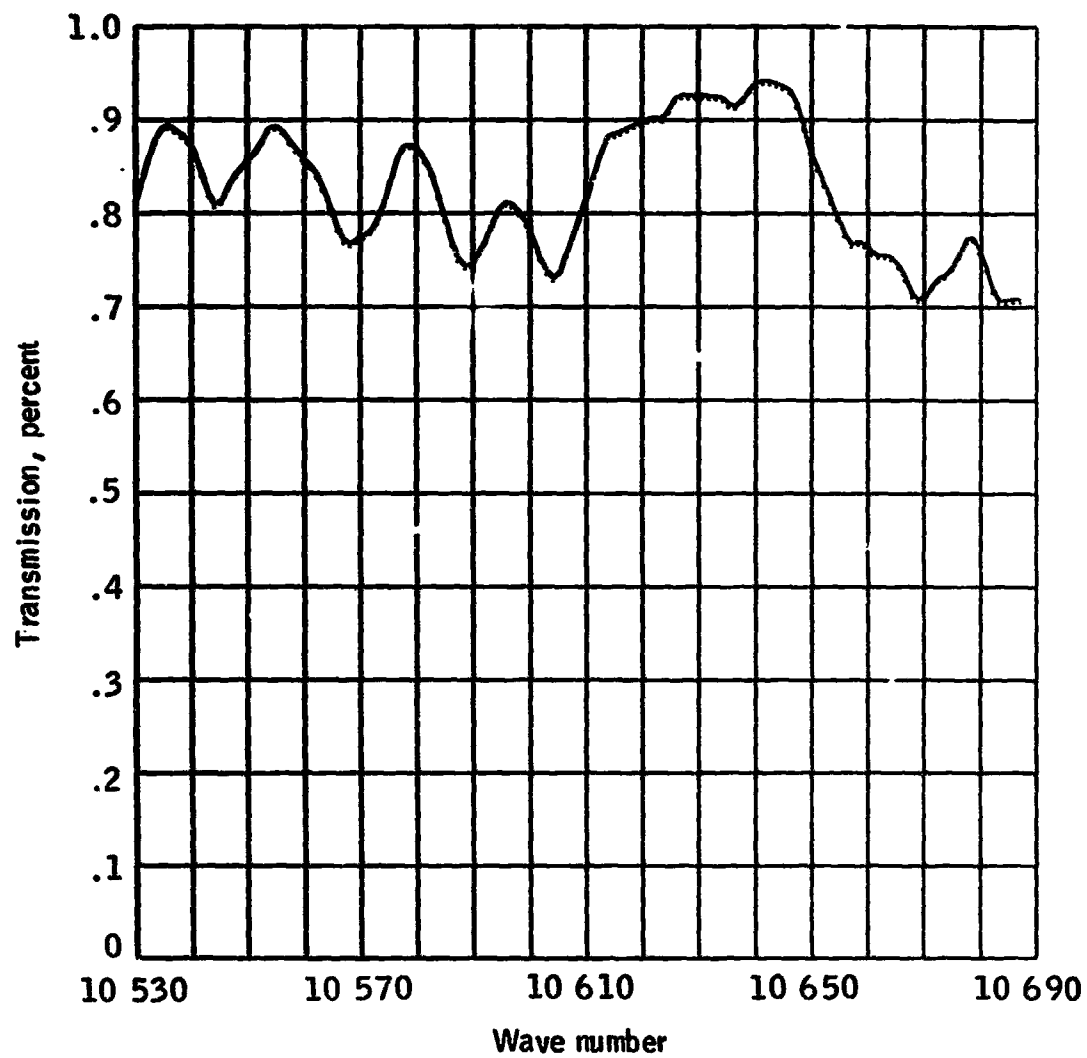1 centimeter$^{-1}$ accuracy.

Figure 4.- Calculated transmission through the atmosphere smoothed by a triangular filter function 20 centimeters$^{-1}$ wide. Albany, N.Y., Jan. 10, 1972, radiosonde, 0.202 centimeter precipitable water.
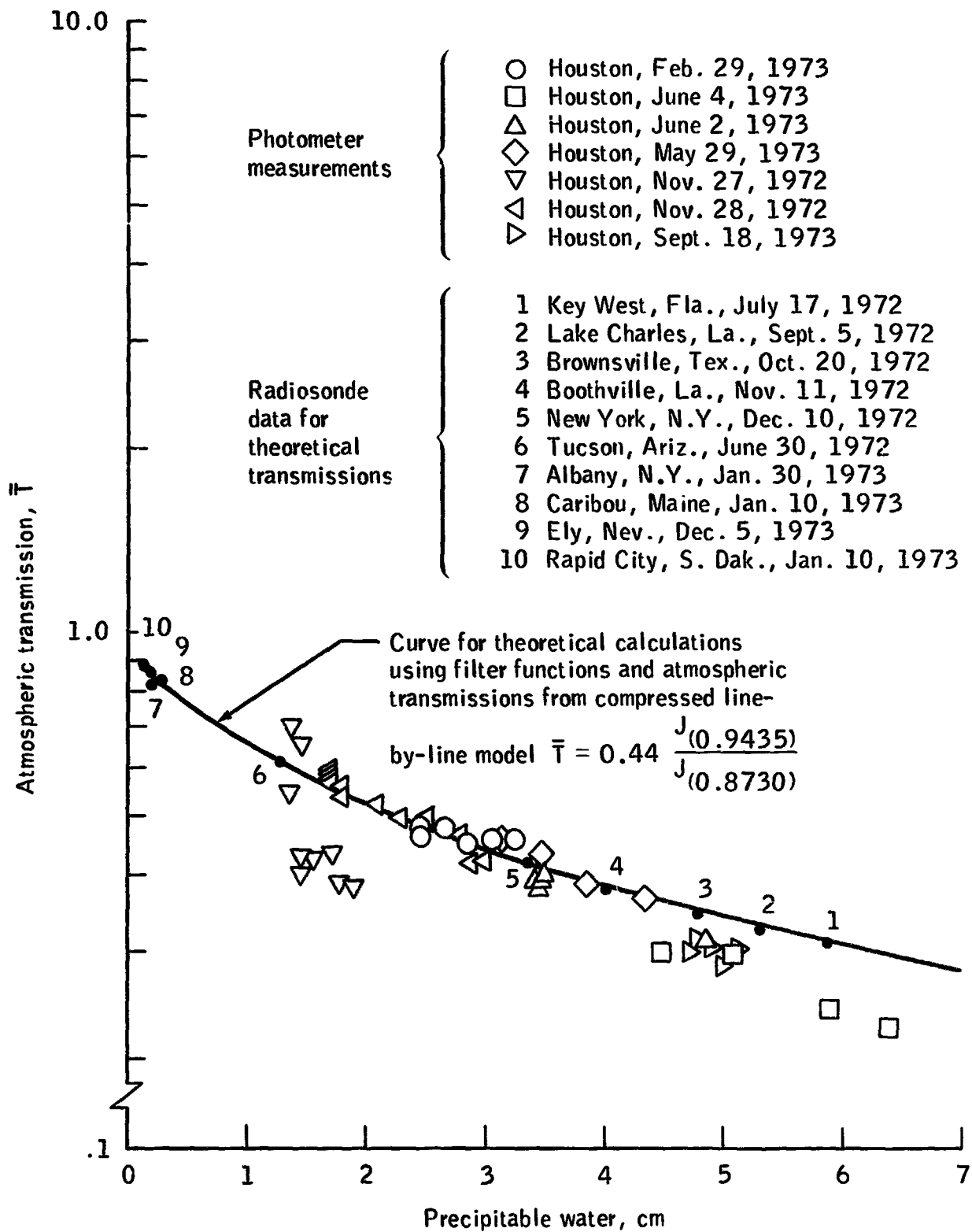
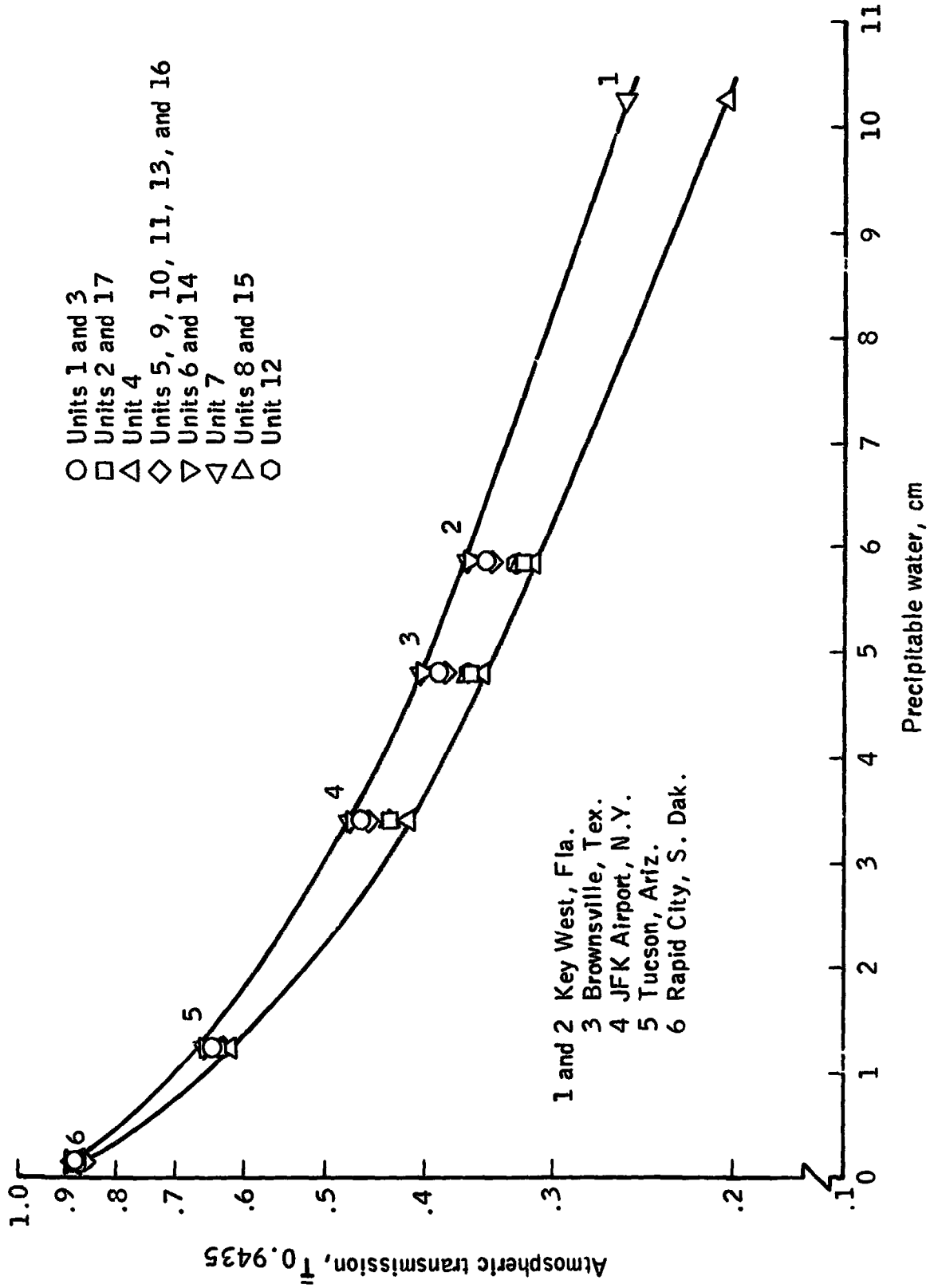Figure 5.— Precipitable water calibration for solar radiometer unit 4.

The figure contains the following legend text:

Photometer measurements:
- ○  Houston, Feb. 29, 1973
- □  Houston, June 4, 1973
- △  Houston, June 2, 1973
- ◇  Houston, May 29, 1973
- ▽  Houston, Nov. 27, 1972
- ◁  Houston, Nov. 28, 1972
- ▷  Houston, Sept. 18, 1973

Radiosonde data for theoretical transmissions:
- 1  Key West, Fla., July 17, 1972
- 2  Lake Charles, La., Sept. 5, 1972
- 3  Brownsville, Tex., Oct. 20, 1972
- 4  Boothville, La., Nov. 11, 1972
- 5  New York, N.Y., Dec. 10, 1972
- 6  Tucson, Ariz., June 30, 1972
- 7  Albany, N.Y., Jan. 30, 1973
- 8  Caribou, Maine, Jan. 10, 1973
- 9  Ely, Nev., Dec. 5, 1973
- 10 Rapid City, S. Dak., Jan. 10, 1973

Curve for theoretical calculations using filter functions and atmospheric transmissions from compressed line-by-line model 

$$\bar{T} = 0.44\ \frac{J_{(0.9435)}}{J_{(0.8730)}}$$

Y-axis: Atmospheric transmission, $\bar{T}$

X-axis: Precipitable water, cm

Figure 6.— Calibration curves for 17 solar radiometers.

Legend (symbols):

○ Units 1 and 3
□ Units 2 and 17
◁ Unit 4
◇ Units 5, 9, 10, 11, 13, and 16
▷ Units 6 and 14
▽ Unit 7
△ Units 8 and 15
○ Unit 12

1 and 2  Key West, Fla.
3  Brownsville, Tex.
4  JFK Airport, N.Y.
5  Tucson, Ariz.
6  Rapid City, S. Dak.

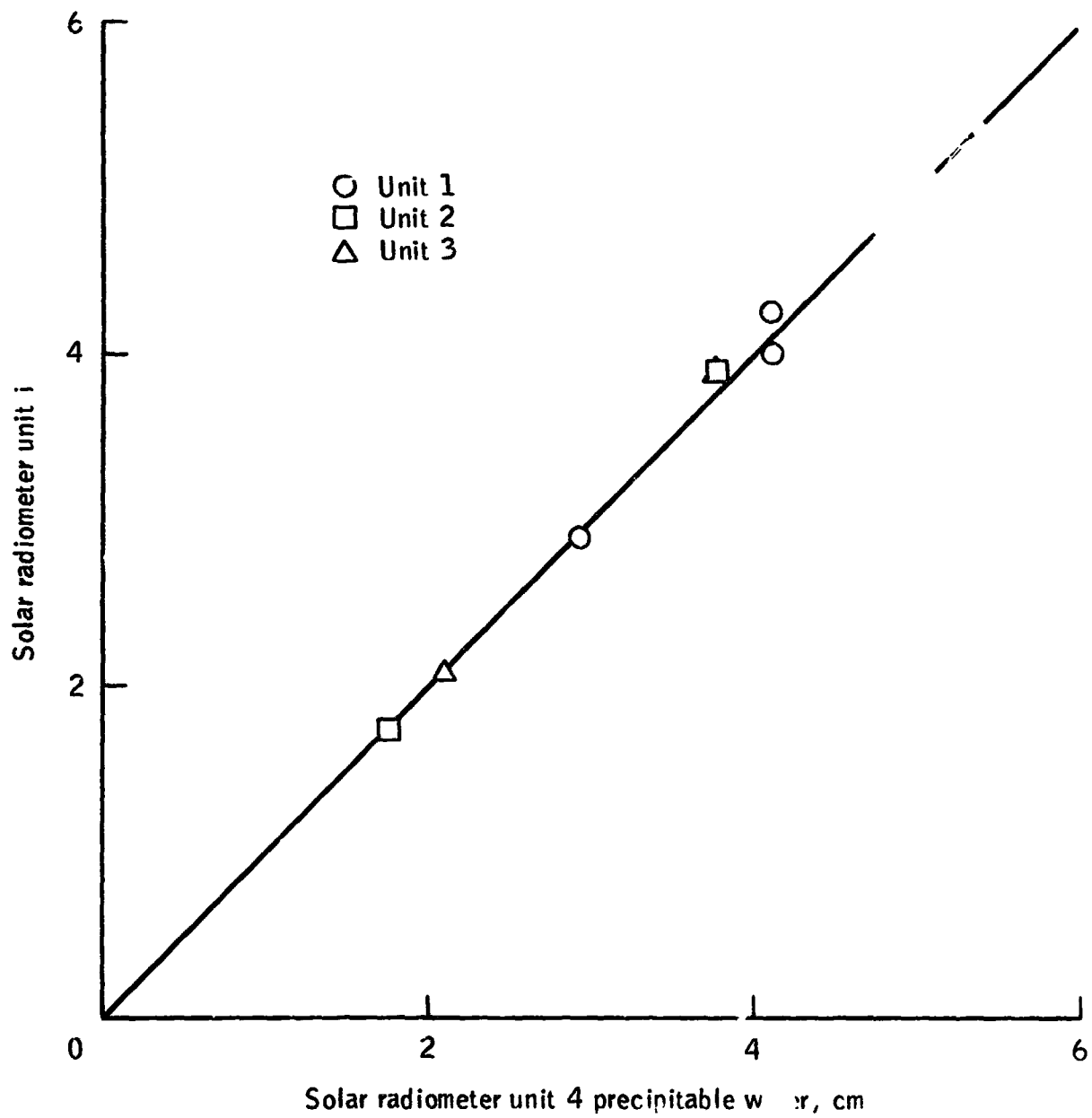X-axis: Precipitable water, cm

Y-axis: Atmospheric transmission, $\bar{T}$ 0.9435

Figure 7.- Calibration verification between solar radiometers.